

## EXAMINATION OF ESTIMATED SURFACE LAYER PROFILES BASED ON SOIL DATA AND MICROTREMOR RECORDS USING OBSERVED SEISMIC GROUND MOTIONS

Nobuo FUKUWA<sup>1</sup> And Jun TOBITA<sup>2</sup>

### SUMMARY

The soil profile is one of the most important factors in earthquake engineering and is closely related to the earthquake damage. A microtremor test is one of the powerful means for inferring the soil profile from the viewpoint of simplicity and cost. In our project, microtremor tests are carried out at the ground surface of 341 locations in Nagoya City, and the horizontal-to-vertical spectral ratios (H/V spectra) of microtremors have been calculated. H/V spectra are classified into seven categories from the viewpoint of the spectral shapes, and soils in Nagoya City are also classified into seven groups from the viewpoint of the topography and the geology based on existing soil data. The relationship between the shapes of H/V spectra and the soil profiles is examined. Then the acceleration Fourier spectra of the seismic ground motions at 48 locations in Nagoya City are also classified into seven groups from the viewpoint of the shapes and the predominant frequencies of Fourier spectra. It is clearly seen that the distribution shape of the acceleration Fourier spectra is very much similar to the shape of the H/V spectra of the same locations. The possibility of estimating the soil profile and predicting the seismic ground motion based on the microtremor observations is pointed out. The estimated depth of the top of the seismic bedrock based on the H/V spectra and the rough average of shear wave velocities has a good accuracy. The estimated depth of the top of the engineering bedrock based on the H/V spectra and the rough average of shear wave velocities is deeper than the depth of the top of the AMA-YATOMI layers. It can be said that the estimated depth corresponds to that of the third gravel layer within the AMA-YATOMI layers.

### INTRODUCTION

The soil profile is one of the most important factors in earthquake engineering and is closely related to the earthquake damage. In the case of 1995 Hyogo-ken Nanbu earthquake, the damage area which is known as "the belt of the earthquake disaster" was formed. A number of investigations have been made to address this characteristic pattern of affected areas [e.g. Kawase et al., 1996]. According to the study results, one of the primary factors is the irregular soil profile of the deep ground that reaches more than 1 kilometer. When considering the seismic design of buildings and the regional earthquake disaster prevention, it becomes important that the soil profile above the bedrock to the ground surface is made clear all over the region and that the characteristics of seismic ground motion is understood in advance. As for the design of structures such as high rise buildings or base-isolated buildings that have natural periods of more than 1 second, availability of deep soil profile is indispensable. Therefore it is necessary to collect existing soil data and to construct databases in the first place.

In Nagoya City, as for shallow soil profile, about 30 PS logging data and about 4000 standard penetration test data are currently open to the public [JGS, 1988]. This data volume is not sufficient because only 1/5 of the city area is covered by the data when the area of Nagoya City is divided into the grid with the grid size of 125 meters by 125 meters. Moreover, most of the borehole data are limited to the depth of piled foundations which is not

<sup>1</sup> Dept of Urban Environment Systems, Faculty of Engineering, Chiba University, Japan Email: ishida@tu.chiba-u.ac.jp

<sup>2</sup> Nagoya University, Nagoya, Japan Fax: +81-52-789-3768

enough. As for the deep soil profile, some investigations such as explosion tests [Masaki et al., 1981], microgravity surveys [Iida and Aoki, 1958], long-period microtremor tests [Miyazaki et al., 1985] have been reported and the soil profile has been approximately estimated. Improvement of the accuracy of the estimated soil profile is expected by conducting dense surveys from these various points of view.

Although there are various ways of finding the soil profile, most of them can not be conducted in large numbers because they are large-scaled and hence expensive. On the contrary, a microtremor test is one of the powerful means for inferring the soil profile from the viewpoint of simplicity and cost. In our project, microtremor tests are carried out at the ground surface in all over the places in Nagoya City, and the horizontal-to-vertical spectral ratios (H/V spectra) of microtremors have been calculated. There is a problem, however, that microtremors are often influenced by the environmental vibration sources such as traffic-induced vibrations. It has been pointed out that the spectral shapes of H/V spectra do not change between day and night and are quite stable [e.g. Nakamura and Ueno, 1986; Tokimatsu and Miyadera, 1992]. In this paper, correlations between the shapes of H/V spectra and the characteristics of existing soil data are examined for Nagoya City, and the possibility of estimating the soil profile based on microtremors are studied based on the earthquake observation data.

## OUTLINES OF OBSERVATION AND DATA TRANSACTION

Microtremor observations have been carried out at 341 locations in Nagoya City as shown in Figure 1. Seismic observations have also been conducted at 48 sites out of these 341 locations. Figure 2 and Table 1 show the information about recent earthquakes occurred near Nagoya. Intensity of both II and IV were observed at 19 locations as shown in Figure 3.

The moving-coil velocity sensors with three coils that have natural periods of 5 seconds are used for the microtremor observations and velocity data in 3 directions (2 orthogonal horizontal components and vertical component) are recorded for 23 minutes at each point. For Analog-Digital conversion, the frequency of 100 Hz is chosen for sampling and the 10 Hz low-pass filter is used for the prevention of anti-aliasing. The resolution of the data recorder is 14 bits. For the analysis in the short-period range, each recorded data is divided into 64 samples with the duration of 20.48 seconds, and the same data is divided into 8 samples with the duration of 163.84 seconds for the analysis in the long-period range. The ensemble average of Fourier amplitude spectra (average spectrum) in each direction is calculated, and the square root of sum of squares of 2 orthogonal horizontal average spectra is calculated as the horizontal average spectrum. The horizontal-to-vertical spectral ratio (H/V spectrum) of microtremor is then calculated using the horizontal average spectrum and the vertical average spectrum. In addition, for the analysis in the long-period range, smoothing of H/V spectrum is done by applying a Parzen window with the width of 0.05 Hz.

## EXAMINATION OF H/V SPECTRUM

Microtremor tests are conducted every hour for 24 hours at one location in the Higashiyama campus of Nagoya University. At the same location, PS logging was conducted and the soil profile above the engineering bedrock ( $V_s=530$  m/sec, 56 m in depth) has been obtained as shown in Table 2. Changes of the shapes of Fourier amplitude spectra (F. S.) and H/V spectra with time are shown in Figures 4 and 5 respectively. It is understood that the H/V spectra are quite stable with time compared to the Fourier amplitude spectra. Figure 6 shows the shear wave amplification spectra at the ground surface against the assumed outcrop response at the base layer calculated by the one dimensional wave propagation analysis using the values listed in Table 2. Figure 7 shows the horizontal-to-vertical amplitude ratio (H/V ratio) of Rayleigh waves. It is possible to say that each H/V spectrum contains not only the fundamental mode but also higher modes of the Rayleigh waves. Therefore, it is possible to say that the H/V spectrum reflects the characteristics of the soil profile.

## CLASSIFICATION OF H/V SPECTRA

H/V spectra are classified into seven categories from the viewpoint of the spectral shapes. The shapes of typical H/V spectra of each category are shown in Figure 8. These are,

Category 1: One peak below the natural period of 1 second which corresponds to the primary natural period of the ground above the seismic bedrock.

Category 2: A clear peak in the long-period range (1 second or more); No peaks in the short-period range with a flat shape.

Category 3: A clear peak in the long-period range; One unclear small peak located next to the long-period peak in the short-period range.

Category 4: A clear peak in the long-period range; Several unclear small peaks located next to the long-period peak in the short-period range.

Category 5: A clear peak in the long-period range; Flat shape between the long-period peak and the short-period peak.

Category 6: A clear peak in the long-period range; A clear large peak in the short-period range.

Category 7: Peaks both in the long-period and in the short-period range; Gentle peaks with a wide foot in the short-period range.

The distribution map of the categorized spectra in Nagoya City is shown in Figure 1 associated with the border between the different soil groups. Soils in Nagoya City are also classified into seven groups from the viewpoint of the topography and the geology based on existing soil data. These are,

An: North of eastern hill; Tertiary deposit; The shallowest seismic bedrock in the city.

As: South of eastern hill; Tertiary deposit.

B: Center of Nagoya; Terrace; Diluvium.

C: North of Nagoya; Delta; Alluvium.

D: West of Nagoya; Reclaimed land; Alluvium.

E: Southwest of Nagoya; Reclaimed land; Alluvium; The deepest seismic bedrock in the city.

F: South of Nagoya; Reclaimed land; Alluvium.

Figure 1 shows a correlation between the distribution of the categorized spectra and the soil groups that are classified based on the topography and geology. The relationship between the categories and the soil profiles is examined at the 6 PS logging locations corresponding to Categories 2~7 of H/V spectra. The soil profile of each location is shown in Figure 9, and the H/V spectrum of microtremor observation together with the shear wave amplification spectra at the ground surface against the assumed outcrop response at the base layer, whose shear wave velocity is 3,000 meters per second, the H/V ratio of fundamental-mode Rayleigh waves and those of higher-modes is shown in Figure 10. In the long-period range, the peak frequency of H/V spectrum corresponds to that of H/V ratio of the fundamental mode of a Rayleigh wave, and to the first natural frequency of the soil layer above the seismic bedrock at each site. In the short-period range, at the sites categorized in Categories 5~7, it is understood that the shapes of H/V spectra are influenced by not only the fundamental mode of the Rayleigh wave but also its higher modes. In the case of Categories 5~7, a clear peak of the H/V spectrum corresponds to the first natural frequency of the ground above the third gravel layer within the AMA-YATOMI layers.

The distribution maps of predominant periods of H/V spectra in the long-period range and predominant frequencies of H/V spectra in the short-period range are shown in Figures 11 and 12 respectively. In the short-period range, only 181 locations out of those categorized as Categories 5~7 are used to draw the map.

## 5. POSSIBILITY OF ESTIMATION OF SOIL PROFILE BASED ON MICROTREMORS

The acceleration Fourier spectra in the E-W direction of the seismic ground motions caused by the earthquakes with the intensity of II and IV (Figure 2 and Table 1), the shear wave amplification spectra computed from the soil profile of the shallower soil above the base with  $V_s=3,000$  m/sec, and the H/V spectra of microtremor observations (at the seismic observation points in Figure 3) are shown together in Figure 13. Figure 13 suggests that the comparison between the seismic ground motion and the microtremor makes a lot of sense when estimating the soil profile. Then the acceleration Fourier spectra of the seismic ground motions at 48 locations in Nagoya City caused by the earthquake with the intensity of IV are also classified into seven groups (An'~F') from the viewpoint of the shapes and the predominant frequencies of Fourier spectra. The shapes of the Fourier spectra of each group are shown in Figure 14, and the shapes of the H/V spectra of each group (An'~F') are

shown in Figure 15. It is clearly seen that the distribution shape of the Fourier spectra is very much similar to the shape of the H/V spectra of the same locations. The distribution map of categorized Fourier spectra is shown in Figure 16 along with the categorized H/V spectra and the boundaries between the different soil groups. Figure 16 shows the possibility of estimating the soil profile and predicting the seismic ground motion based on the microtremor observations.

Figure 17 shows the estimated depth of the top of the seismic bedrock, which is evaluated based on the predominant period of H/V spectra in the long-period range (See Figure 11) and the average S wave velocity of the ground above the seismic bedrock. As the average S wave velocity, 1,000 m/sec is used for the groups An and B, 900 m/sec is used for the groups C and D, and 1,200 m/sec is used for the groups As, E and F based on the existing soil data. Figure 18 shows the depth of the top of the seismic bedrock estimated from the existing soil data (explosion tests, microgravity surveys and deep wells) [Aichi Pref., 1993]. It is understood that the estimated depth of the top of the seismic bedrock based on the H/V spectra and the rough average of shear wave velocities has a good accuracy. Figure 19 shows the estimated depth of the top of the engineering bedrock, which is evaluated by considering the predominant frequency of H/V spectra in the short-period range (See Figure 12) and the average S wave velocity of 280 m/sec of the ground above the third gravel layer within the AMA-YATOMI layer. Figure 20 shows the depth of the top of the AMA-YATOMI layer [JGS, 1988]. It is pointed out that the estimated depth of the top of the engineering bedrock based on the H/V spectra and the rough average of shear wave velocities is deeper than the depth of the top of the AMA-YATOMI layers. Thus, it can be said that the estimated depth corresponds to that of the third gravel layer within the AMA-YATOMI layers.

## CONCLUSIONS

In this paper, the relationship between the shapes of H/V spectra of microtremor observations and the soil profiles is examined. Then the distribution shape of categorized H/V spectra is compared with that of categorized acceleration Fourier spectra. The possibility of estimating the soil profile and predicting the seismic ground motion based on the microtremor observations is pointed out. The estimated depth of the top of the seismic bedrock and the engineering bedrock (the third gravel layer within the AMA-YATOMI layers) based on the H/V spectra and the rough average of shear wave velocities have good accuracy.

## ACKNOWLEDGMENTS

The authors wish to thank Mr. Hirohito Takahashi, Mr. Masanori Iida and Mr. Hitoshi Nakamura of Nagoya University, and Oyo Corporation for conducting the field observations and processing the data. The authors also wish to thank K-Net, Aichi Prefecture, Nagoya City, Toho Gas and Chubu Electric Power Corporation for providing the valuable data.

## REFERENCES

- Aichi Pref. (1993), *The reports of damage prediction against Tokai earthquake in Aichi Prefecture* (in Japanese).
- Arakawa, M., Fukuwa, N., Ishida, E. and Koide, E. (1996), 'A study on the use of soil information to evaluate seismic ground motion', *Proc. of the 19th symposium on computer technology of information, systems and applications*, pp343-348 (in Japanese).
- Iida, K. and Aoki, H. (1958), 'Gravity anomalies and the corresponding subterranean mass distribution with special reference to be the Nobi plain and its vicinity', *Japan, J. Earth Sci., Nagoya Univ.*, Vol.6, No.2, pp113-142.
- The Japanese Geotechnical Society, Chubu branch (1988), *Geotechnical Data of Subsoils in Nagoya (New edition)* (in Japanese).
- Kawase, H. and Hayashi, Y. (1996), 'Strong motion simulation in Chuo ward, Kobe, during the Hyogo-ken Nambu earthquake of 1995 based on the inverted bedrock motion', *Journal of Struct. Constr. Engng, AIJ*, No.480, pp67-76 (in Japanese).
- Masaki, K., Taniguchi, H. and Iida, K. (1981), 'On the ground structure of Nagoya area II - Observations of seismic waves generated from the 2nd Nagoya-Nabeta and the 1st Toyohashi-Tahara explosions -', *Research reports in Aichi Institute of Technology*, pp159-171 (in Japanese).

Miyazaki, T., Taga, N., Togashi, Y., Taniguchi, H. and Imaoka K. (1985), 'Synthetic research of microseisms in the Nohbi plain - Comparison of observational results with vibrational analysis -', *Journal of Struct. Constr. Engng, AIJ*, No.351, pp103-112 (in Japanese).

Nakamura, Y. and Ueno, M. (1986), 'A simple estimation method of dynamic characteristics of subsoil', *Proc. the 7th Japan Earthq. Engrg. Symp.*, pp265-270 (in Japanese).

Tokimatsu, K. and Miyadera, Y. (1992), 'Characteristics of Rayleigh waves in microtremors and their relation to underground structures', *Journal of Struct. Constr. Engng, AIJ*, No.439, pp81-87 (in Japanese).

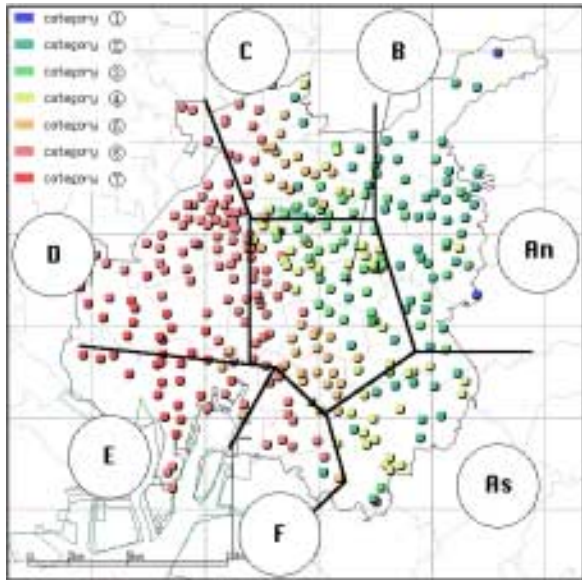


**Figure 1: Observation locations of microtremors in Nagoya**



**Figure 2: Hypocenters of recent earthquakes**



**Figure 3: Seismic observation locations in Nagoya**

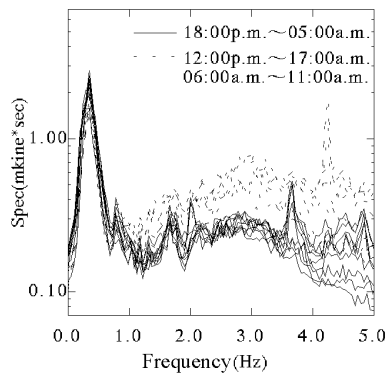


**Figure 4: Changes of Fourier amplitude spectra with time (N-S direction)**

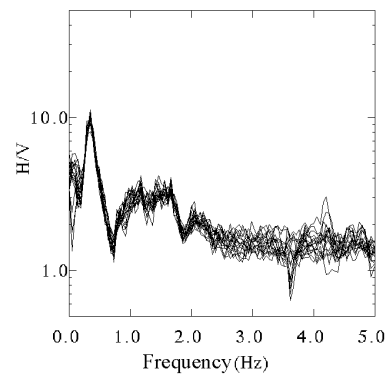


**Figure 5: Changes of H/V spectra with time**

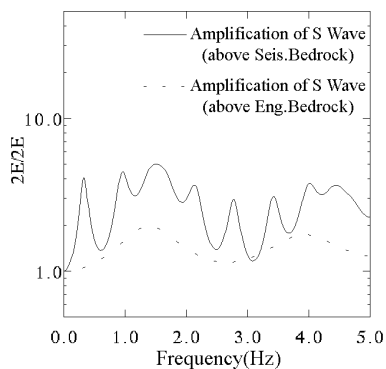


**Figure 6: Amplification of S wave above base layer**

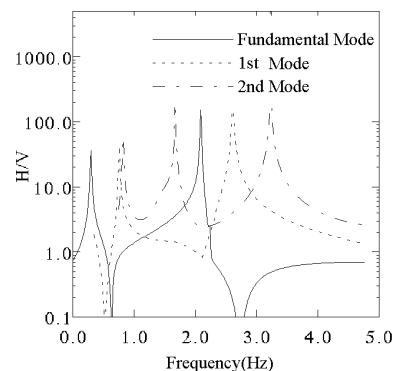


**Figure 7: H/V amplitude ratio of Rayleigh waves**

**Table 1: Information about recent earthquakes**

	Date	Hypocenter (N. Lat., E. Long.)	Depth	Epicentral Distance	Magnitude
I	1996.10.5	( 35.0, 138.0 )	26 km	97 km	4.4
II	1997.3.16	( 34.9, 137.5 )	39 km	56 km	5.8
III	1998.2.10	( 35.7, 137.1 )	10 km	61 km	4.3
IV	1998.4.22	( 35.1, 136.6 )	10 km	30 km	5.4
V	1998.12.2	( 35.1, 136.6 )	40 km	34 km	3.9

**Table 2: Soil profile in Nagoya University**

Depth (m)	Thickness (m)	S Wave Velocity (m/s)	Bulk Density (g/cm <sup>3</sup> )	Impedance Ratio
4.0	4.0	180	1.7	1.00
8.0	4.0	220	1.7	1.22
33.0	25.0	280	1.8	1.48
39.0	6.0	320	1.8	1.24
48.0	9.0	300	1.8	1.12
49.0	1.0	530	2.0	2.15
53.5	4.5	530	1.9	2.00
54.5	1.0	530	2.0	1.94
56.0	1.5	530	2.0	1.91
497.6	441.6	700	2.0	2.46
755.9	258.4	1600	2.0	2.45
756.9	1.0	3000	2.0	3.07

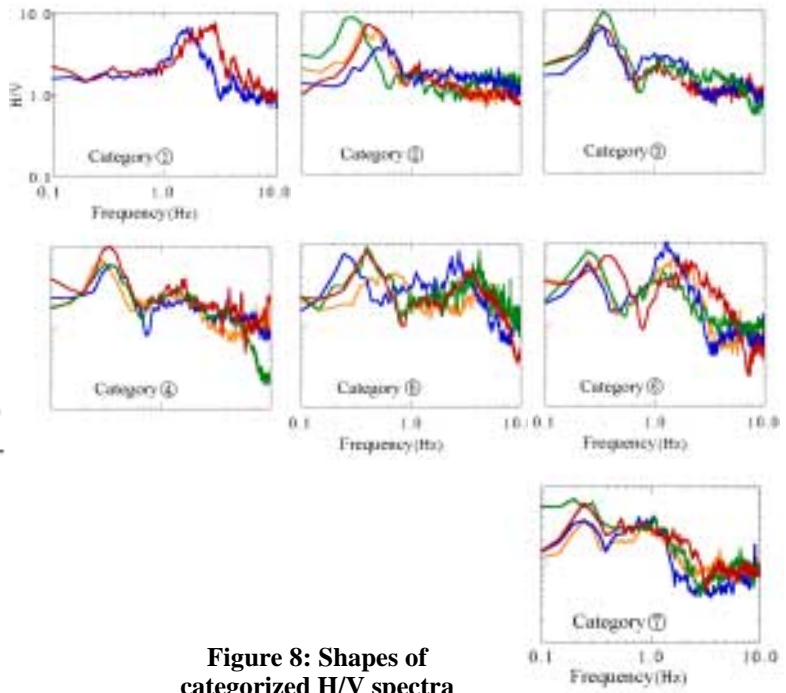


**Figure 8: Shapes of categorized H/V spectra**

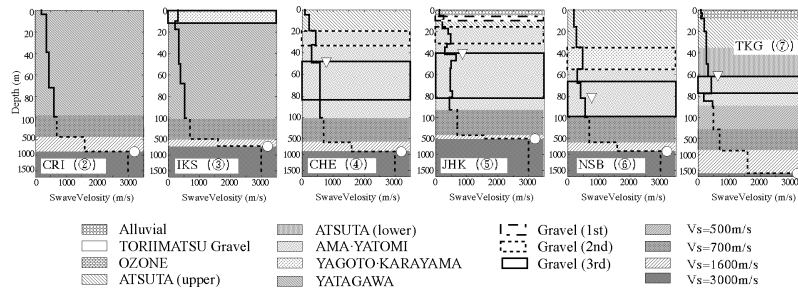


**Figure 9: Soil profiles of 6 PS logging locations**

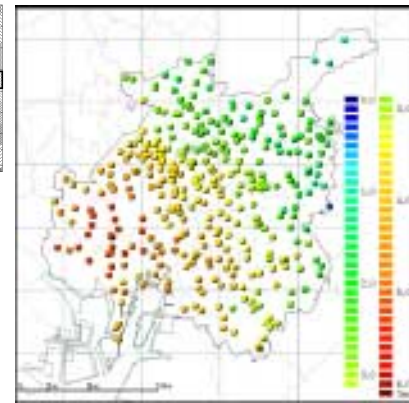


**Figure 11: Predominant periods of H/V spectra**

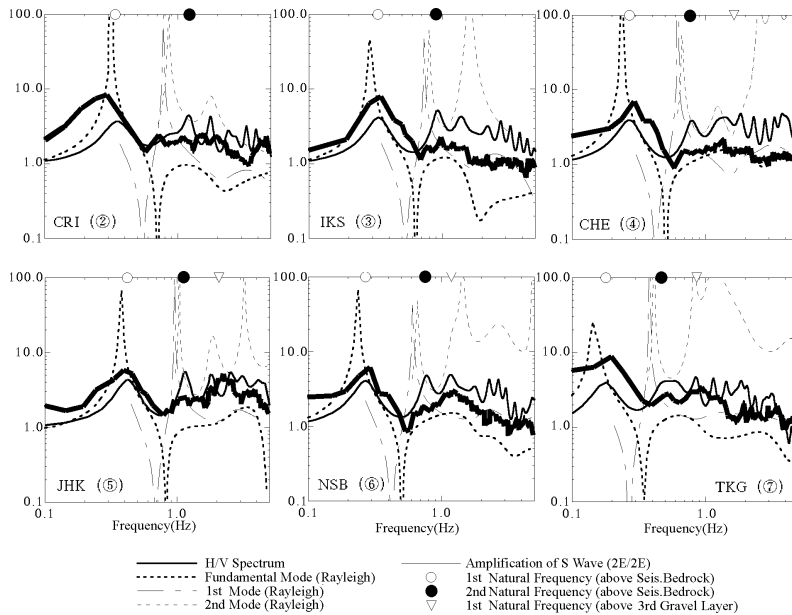


**Figure 10: H/V spectra of microtremor observations, S wave amplification spectra above seismic bedrock**

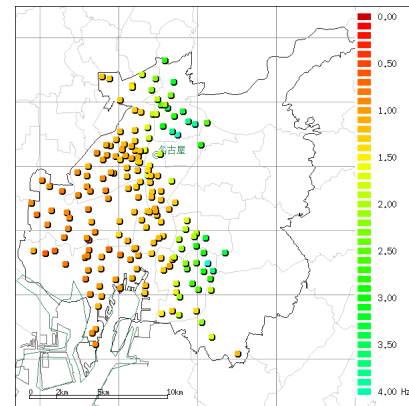


**Figure 12: Predominant frequencies of H/V spectra**

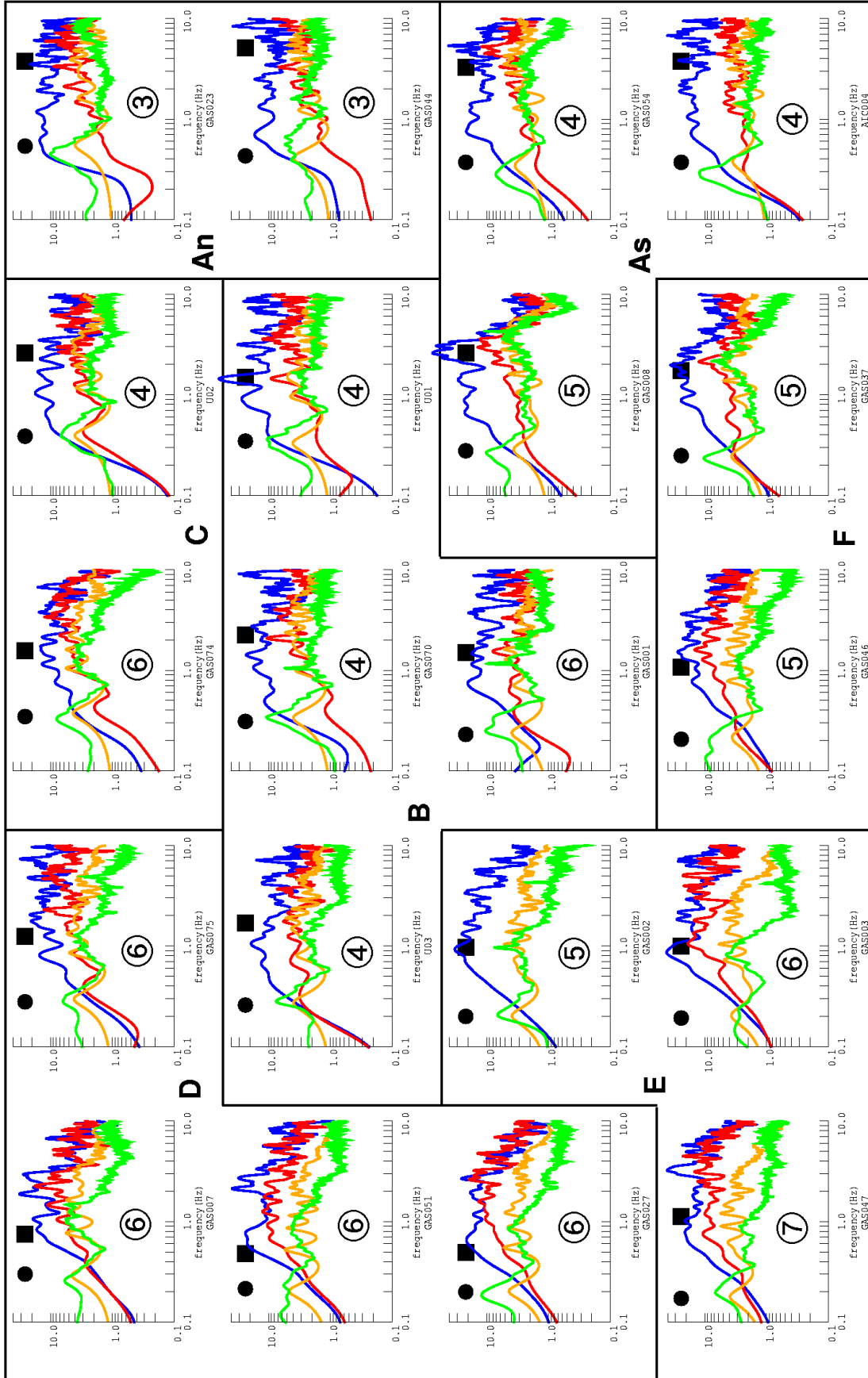


Figure 13: Acceleration Fourier spectra of seismic ground motions (blue lines: II; red lines: IV), S wave amplification spectra above seismic bedrock (orange lines) and H/V spectra of microtremor observations (green lines)

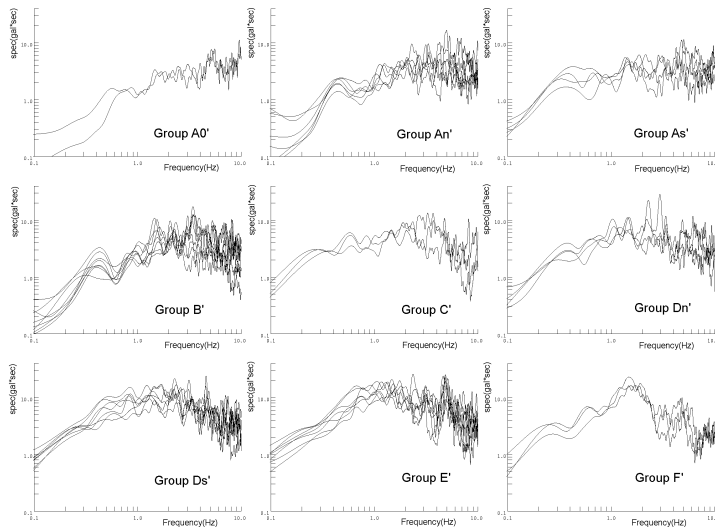


Figure 14: Shapes of acceleration Fourier spectra of each group

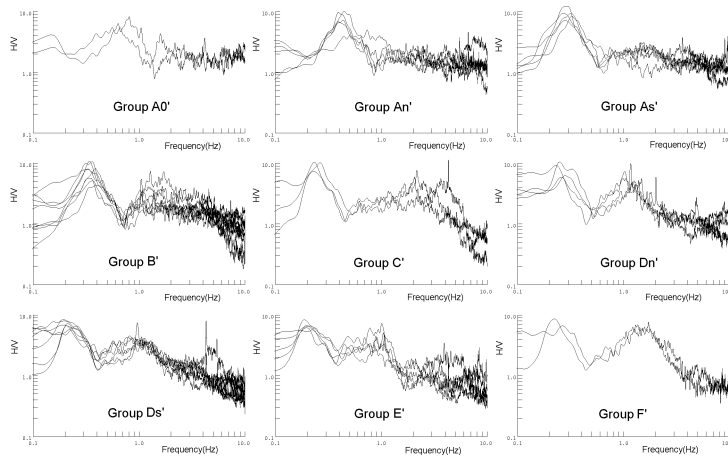


Figure 15: Shapes of H/V spectra of each group

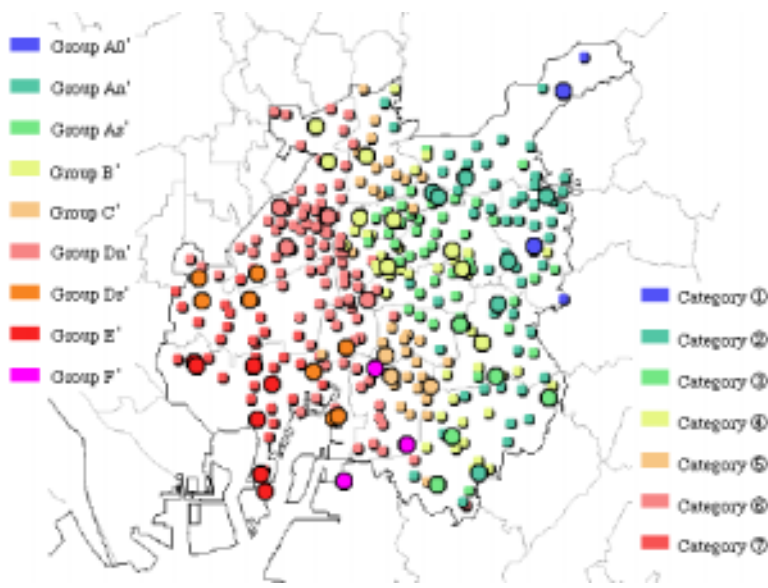


Figure 16: Distribution of categorized acceleration Fourier spectra and H/V spectra along with boundaries between different soil groups

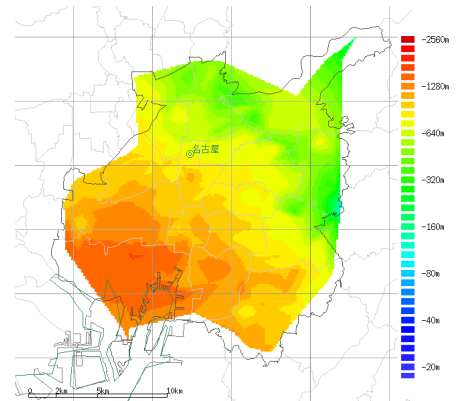


Figure 17: Estimated depth of top of seismic bedrock

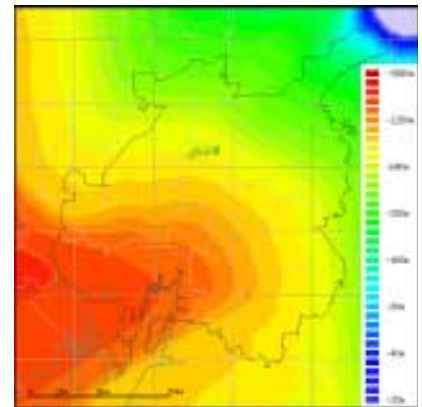


Figure 18: Depth of top of seismic bedrock

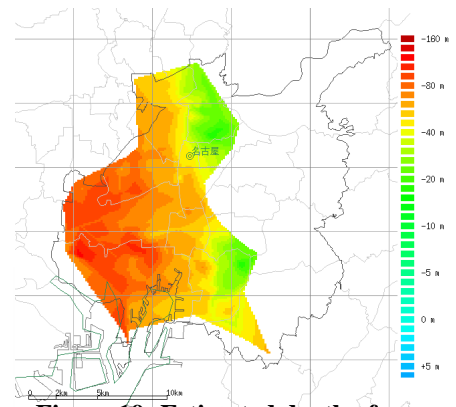


Figure 19: Estimated depth of

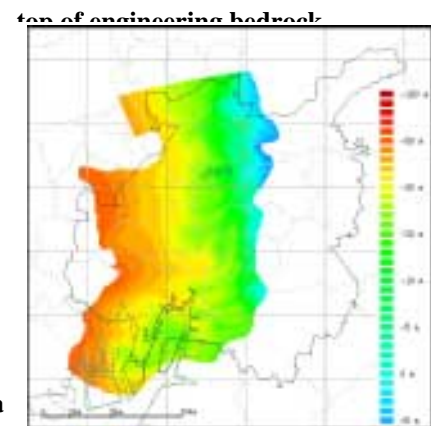


Figure 20: Depth of top of AMA-YATOMI layer